Hard and soft pomerons in elastic nucleon scattering

O. V. Selyugin

BLTPh, JINR, Dubna, Russia

Abstract

An analysis of the possible contribution of the hard pomeron in elastic hadron scattering at LHC energies is made. It is shown that such a contribution has affected the shape of the differential cross section in the Coulomb-hadron interference region and in the dip region. On the basis of the new High-Energy General Structure (HEGS) model, the possible contributions of the hard pomeron are investigated. The predictions of the model at 8 TeV are discussed.

Keywords: Hadron, pomeron, odderon, elastic scattering, high energies

1. Introduction

The successful work of the LHC at 7 TeV is in most part connected to inelastic processes. In these processes we hope to find an answer to many old questions of hadron physics. However, the dynamics of strong interactions finds its most complete representation in elastic scattering at small angles. Only in this region of interactions we can measure the basic non-perturbative properties of the strong interaction which defines the hadron structure: the total cross section, the slope of the diffraction peak and the parameter $\rho(s,t)$ - the ratio of the real part to the imaginary part of the scattering amplitude. Their values are connected, on the one hand, with the large-scale structure of hadrons and, on the other hand, with the first principles which lead to the theorems on the behavior of the scattering amplitudes at asymptotic energies [1, 2].

The preliminary data of the TOTEM Collaboration [3] are inconsistent with most existing predictions [4, 5, 6]. They lead to different predictions for the structure of the scattering amplitude at asymptotic energies, where the diffraction processes can display complicated features [7]. This especially concerns the asymptotic unitarity bound connected with the Black

Disk Limit (BDL) [8]. Recently, there appeared some new works [9, 10, 11] to understand the physics of elastic scattering at LHC energies. The impact of the hard pomeron contribution on the elastic differential cross sections is very important for understanding the properties of the QCD in the non-perturbative regime [12]. In [13] it is indeed suggested that such a contribution of the hard pomeron can explain the preliminary result of the TOTEM Collaboration [3] on the elastic proton-proton differential cross sections at 7 TeV.

The hard pomeron which is obviously present in inelastic diffractive processes with a large intercept $1 + \epsilon_2 \approx 1.4$ [14] will lead to the appearance of the saturation BDL-regime at somewhat low energies. It is not obvious how the total cross sections will grow with energy, especially in the energy region of the LHC. In the present work, we investigate the impact of the hard pomeron on some features of elastic proton-proton scattering at LHC energies and at small momentum transfer. The large intercept of the hard pomeron leads to a large real part of the scattering amplitude. The impact of the real part on the form of the differential cross sections is in most part reflected in the dip region, where the imaginary part of the scattering amplitude has a zero, and in the Coulomb-hadron interference region at small momentum transfer, where the size of the real part determines the size and sign of the Coulomb-hadron interference term. The situation is complicated by the possible transition to the saturation regime, as the BDL is reached at the LHC [15]. The effect of saturation will be a change in the t dependence of $B(s,t)$ and $\rho(s,t)$, which will begin for $\sqrt{s} = 2$ to 6 TeV and which may drastically change $B(t)$ and $\rho(t)$ at $\sqrt{s} = 14$ TeV [16].

In the paper, we examine and compare the contribution of the soft and hard pomerons to the differential cross sections. First, we analyze this contribution in a purely phenomenological representation. We pay special attention to the Coulomb-hadron interference region. This is tightly connected with the problems of the determination of the value of $\rho(s, t = 0)$ and of the value and energy dependence of the total cross sections, as the assumption about the form of elastic scattering amplitude seriously impacts on the determination of both values [17].

Then we examine the possible hard pomeron contribution in the framework of our high-energy general structure (HEGS) model [18] which takes into account two different hadronic form factors calculated from the first and second moment of the general parton distributions (GPDs) [19].

In this model, the real part of the hadronic amplitude is determined

through the use of a complex s, and the amplitude satisfies crossing symmetry. The quantitative description of all existing experimental data at $52.8 \leq \sqrt{s} \leq 1960$ GeV, including the Coulomb range and large momentum transfers $0.0008 \leq |t| \leq 9.75$ GeV^2 , is obtained with only 3 fitted high-energy parameters. The comparison of the predictions of the model at 7 TeV and preliminary data of the TOTEM collaboration are shown to coincide well. In the framework of this model, only the Born term of the scattering amplitude is introduced. Then the whole scattering amplitude is obtained as a result of the unitarization procedure of the hadron Born term that is then summed with the Coulomb term. The Coulomb-hadron interference phase is also taken into account [20, 21, 22]. The essential feature of the model is that both parts of the Born term of the scattering amplitude have a positive sign, and that the diffraction structure is determined by the unitarization procedure.

2. Hard pomeron and size of $\rho(s,t)$

Usually, the value of $\rho(s, t = 0)$ is assumed to be small and to vary little with s at high energies: $\rho(s, t = 0) \approx 0.14$ at $\sqrt{s} = 541$ GeV and 7 TeV. The impact of the real part of the scattering amplitude is most profound at small $|t|$ and in the region of the diffraction minimum which is determined by the zero of the imaginary part of the scattering amplitude. It is supposed that the odderon contribution makes the sharpest dip in the case of pp scattering and fills it in the case of $p\bar{p}$ scattering at $\sqrt{s} = 52.8$ GeV and $\sqrt{s} = 541 \div 1980$ GeV. In this case, we can expect a large dip in the case of the pp scattering at LHC energies. The number of elastic events is related to the total hadronic cross section through the following formula:

$$
\frac{dN}{dt} = \mathcal{L} \left[\frac{4\pi\alpha^2}{|t|^2} G^4(t) - \frac{2\alpha \left(\rho(s,t) + \phi_{CN}(s,t) \right) \sigma_{tot} G^2(t) e^{-\frac{B(s,t)|t|}{2}}}{|t|} \right.
$$
$$
\left. + \frac{\sigma_{tot}^2 (1 + \rho(s,t)^2) e^{-B(s,t)|t|}}{16\pi} \right]
\tag{1}
$$

where the three terms are due to Coulomb scattering, Coulomb-hadron interference and hadronic interactions. $\mathcal{L}$ is the integrated luminosity, α is the electromagnetic coupling constant, $\phi_{CN}(s,t)$ is the Coulomb-hadron phase, and $G(t)$ is the electromagnetic form factor given by

$$
G(t) = \frac{4m_p^2 - \mu t}{4m_p^2 - t} \frac{\Lambda^2}{(\Lambda - t)^2}.
\tag{2}
$$

3

with m_p the proton mass, $\Lambda = 0.71 \, \text{GeV}^2$ and $\mu = 2.79$.

The differential cross sections at small momentum transfer $|t| \leq 0.05 \, \text{GeV}^2$, in the so-called Coulomb-hadron interference region, are determined by the interference of the Coulomb amplitude with the real part of the hadron amplitude. Hence, the s and t dependences of the real part of the hadron amplitude, which is reflected in $\rho(s,t)$, will determine the form of the differential cross sections.

Let us take the hard pomeron as a simple pole, in the conventional form

$$F_{hpom.}(s,t) \;=\; H_{hpom.} \hat{s}^{\epsilon_2} \, e^{\alpha_2'(\ln[\hat{s}] \; t}; \tag{3}$$

with $\epsilon_2 = 0.4$ and $\alpha_2' = 0.1$ and the soft pomeron in the same form with parameters $\epsilon_1 = 0.11$ and $\alpha_1' = 0.24$, and

$$\hat{s} = s \, e^{-i\pi/2}/s_0; \quad s_0 = 1 \, \text{GeV}^2. \tag{4}$$

In this case, the Born term of the elastic hadron scattering amplitude which takes into account the soft and hard pomerons is

$$F_h^B(s,t) \;=\; G^2(t) \, [F_{spom.}(s,t) + F_{hpom.}(s,t)]; \tag{5}$$

where $t = -q^2$ is the momentum transfer and $G(t)$ is the Sachs form factor. Such a simple phenomenological picture is appropriate at very high energies, where the other Reggeon contributions are very small. We take the ratio of the hard and soft constant, as in [13], $H_{hpom.}/H_{spom.} = 1/250$.

To obtain the full hadron scattering amplitude, we use the eikonal approximation [23, 24, 25, 26, 27, 28]. So, first, we have to calculate the eikonal phase and then the whole unitarized amplitude

$$\chi(s,b) \;=\; \frac{1}{2\pi} \int d^2q \; e^{i\vec{b}\cdot\vec{q}} \, F_h^B(s,q). \tag{6}$$

$$F_h(s,t) \;=\; \frac{i}{2\pi} \int d^2q \; e^{i\vec{b}\cdot\vec{q}} \, (1 - \exp[-\chi(s,b)]). \tag{7}$$

First, let us examine the Born term of the hard pomeron contribution at small $|t|$. The size of $\rho(s, t = 0)$ will be 0.14 for the soft pomeron and 0.73 for the hard pomeron and change little with t (Fig. 1,left panel). If we unitarize the amplitude using the eikonal representation, the size of $\rho(s,t)$
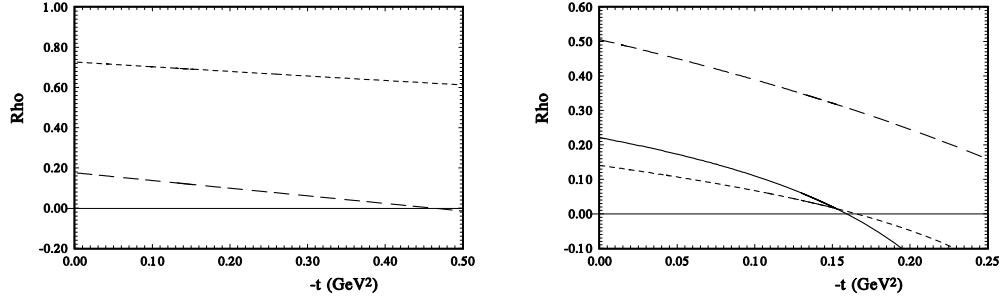
4

Figure 1: Left panel: $\rho(s, t = 0)$ from the Born amplitude of the soft and hard pomerons (short- and long-dashed lines); Right panel: the same after the eikonalization of the Born amplitude (plain lines - the some of the soft and hard pomerons) at 8 TeV with the ratio of the $H_{hard}/H_{soft} = 0.005$
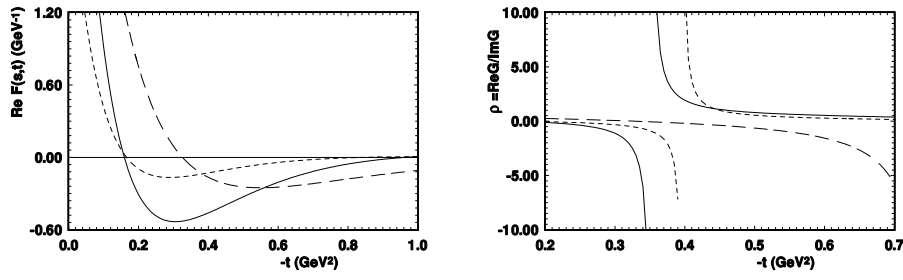

Figure 2: After the eikonalization at $\sqrt{s} = 8$ TeV - Left panel: $ReF(s,t)$ and Right panel - $\rho(s,t)$ (short-dashed line - soft pomeron; long-dashed line - hard pomeron; plain line - sum of soft and hard pomerons).
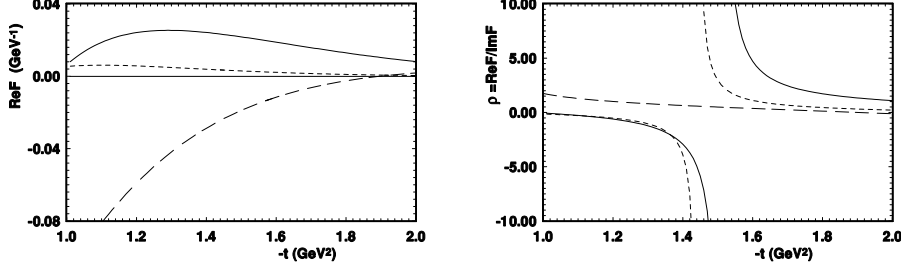
Figure 3: After eikonalization at $\sqrt{s} = 8$ TeV - Left panel: $ReF(s,t)$ and Right panel: $\rho(s,t)$ (short-dashed line - soft pomeron; long-dashed line - hard pomeron; plain line - sum of soft and hard pomerons).

changes faster with t, and the sum of the soft and hard pomerons increases the size of $\rho(s, t = 0)$ to 0.23 (Fig. 1,right panel). Hence, such an increase in the real part has to have an impact on the form of the differential cross sections in the Coulomb-hadron region.

Now let us see what impact the hard pomeron contribution has on the t - dependence of the real part and on $\rho(s,t)$, after the eikonalization of the corresponding Born amplitude. There are two regions where $\rho(s,t)$ changes its sign. The first appears in the region of $|t| \sim 0.5$ GeV^2. The behavior of the real part and $\rho(s,t)$ is shown in Fig. 2. It is clear that the presence of a small hard pomeron contribution changes the t dependence of the real part and of $\rho(s,t)$.

Figure 3 (left panel) shows the result of the calculation of the real part of the scattering amplitude in the region where the imaginary part, obtained after eikonalization of the sum of the soft and hard pomeron, changes its sign. We see that despite the fact that the soft pomeron has a small contribution in this t region and that the hard pomeron has a large negative contribution, their sum of has a positive sign and a rather large value. So the presence of a hard pomeron will significantly change the size and position of the diffraction minimum. This can be seen in Fig. 3 (right panel) where the value of $\rho(s,t)$ is presented in the region of the diffraction minimum. The position of the diffraction minimum moves to larger momentum transfer.

Let us examine how the form of the Coulomb-hadron interference term in the differential cross sections changes with the presence of the hard pomeron. For proton-proton scattering, this term has a negative sign in the region
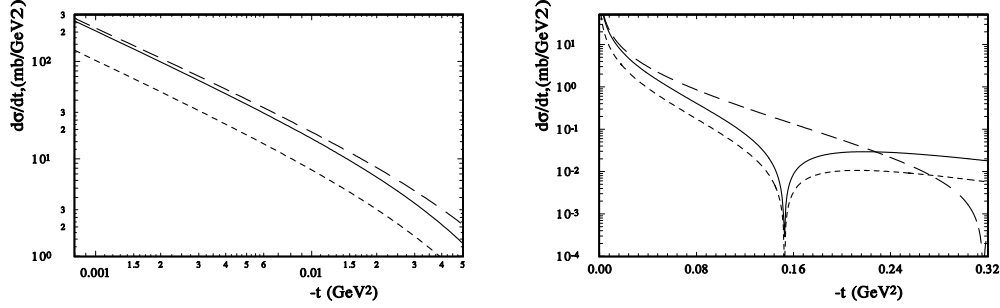
6

Figure 4: The contribution to $d\sigma/dt$ of the CNI term by module at $\sqrt{s} = 8$ TeV - Left panel: $ReF(s,t)$ and Right panel - middle t (short dashed line - soft pomeron; long-dashed line - hard pomeron; solid line - sum of soft and hard pomerons).

where the real part of the hadron scattering amplitude is positive.

This contribution to the differential cross section is shown in Fig. 4. It has a negative sign and the figure shows its absolute value. In the Coulombic-nuclear interference (CNI) region, i.e. at very small momentum transfer, the contribution essentially increases the size of this term and has a negative sign. At larger momentum transfer the sum of the soft and hard pomerons leads to a change of sign of the CNI term at low t value. This zero leads to a "break" in the differential cross section.

3. High-Energy General-Structure model of hadron interactions

In various models, we can obtain a different picture of the profile function based on a different representation of the hadron structure. In our model [18], we suppose that the elastic hadron scattering amplitude can be divided into two pieces. One is proportional to the electromagnetic form factors. It plays the most important role at small momentum transfer. The other piece is assumed to be proportional to the matter distribution in the hadron and plays the most important role at large-momentum transfer.

The Born term of the elastic hadron amplitude can be written as

$$
\begin{aligned}
F_h^{Born}(s,t) = \quad & h_1 \, G^2(t) \, F_a(s,t) \, (1 + r_1/\hat{s}^{0.5}) \\
+ \quad & h_2 \, A^2(t) \, F_b(s,t) \, (1 + r_2/\hat{s}^{0.5})
\end{aligned}
\tag{8}
$$

7

where $F_a(s,t)$ and $F_b(s,t)$ are

$$F_a(s,t) \; = \; \hat{s}^{\epsilon_1} \; e^{B(s) \; t}; \quad F_b(s,t) \; = \; \hat{s}^{\epsilon_1} \; e^{B(s)/4 \; t}; \tag{9}$$

with $\hat{s}$ as eq.(4): $\hat{s} = s \; e^{-i\pi/2}/s_0; \quad s_0 = 1 \; \text{GeV}^2$. The electromagnetic form factors can be represented as the first moments of GPDs following from the sum rules [29, 30]. Hence, we take $F_1^q(t)$ as the conventional electromagnetic form factor (2) and the second form factor is presented in the form

$$A(t) = L_2^4 \; (L_2^2 - t)^{-2}; \tag{10}$$

where $L_2^2 = 2 \; \text{GeV}^2$ is determined from the integral of the second moment of the GPDs. Note that the form of the GPDs is itself determined by deep-inelastic processes and by the measurement of the electromagnetic form factor from electron-nucleon elastic scattering. Hence, the form of the electromagnetic form factor determines the form of the second form factor. The discussion of the energy-momentum structure form factors of particles has a long history, see for example [31, 32]. Of course, the correlation of the strong interaction with the electromagnetic density and matter density is an assumption. However, the HEGS model gives a good description of the experimental data with a minimum of free parameters.

The slope of the scattering amplitude has the standard logarithmic dependence on energy $B(s) = \alpha' \; ln(\hat{s})$ with $\alpha' = 0.24 \; \text{GeV}^{-2}$. The final elastic hadron scattering amplitude is obtained after unitarization of the Born term.

As a result, our model has only 3 free high-energy parameters which we obtained by fitting the existing experimental data with 3 high-energy parameters $h_1 = 1.09 \pm 0.004; \quad h_2 = 1.57 \pm 0.006; \epsilon_1 = 0.11$ and 2 low-energy parameters $r_1^2 = 1.57 \pm 0.02; \quad r_2 = 5.56 \pm 0.06$. We used all the existing experimental data at $\sqrt{s} \geq 52.8 \; \text{GeV}$, including the whole Coulomb-hadron interference region, and all data to the maximum momentum transfer. In the fitting procedure, only statistical errors were taken into account in the χ^2. The systematic errors were used as an additional normalization of the experimental data of one experiment as a whole [18].

As an example, in Fig. 5, the differential cross sections for proton-antiproton elastic scattering at $\sqrt{s} = 1960$ GeV and predictions for 7 and 8 TeV for proton-proton scattering are presented. We see the filling of the diffraction minimum in the case of $p\bar{p}$ scattering and only a partial filling of the minimum for pp scattering. Now in the HEGS model we obtained a good description of the region of the diffraction minimum at the energy
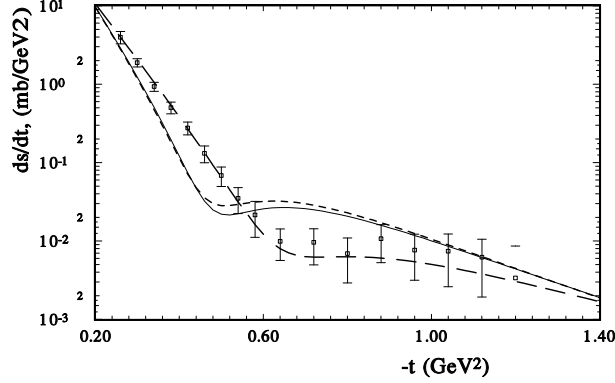
Figure 5: $d\sigma/dt$ in $p\bar{p}$ elastic scattering at $\sqrt{s} = 1960$ GeV (long-dashed line: fit of the model) and experimental data [33]; predictions of the model for pp elastic scattering at 7 TeV (solid line) and 8 TeV (dashed line).

$52.8 \leq \sqrt{s} \leq 1960$ GeV for pp and $p\bar{p}$ scattering. However, we have not a good description of the dip region for $p\bar{p}$ scattering at $\sqrt{s} = 52.8$ GeV [18]. Maybe a larger difference can be obtained if we take into account the odderon contribution.

In Fig. 6 the descriptions by the model of the experimental data for proton-antiproton scattering at $\sqrt{s} = 52.8$ and 541 GeV and the predictions for proton-proton scattering at 7 and 8 TeV are shown. Clearly, the model describes the experimental data in the Coulomb-hadron interference region well. In this case, the Coulomb-hadron interference term is large, especially at $\sqrt{s} = 541$ GeV as t is very small. The good description of the experimental data shows that the energy dependence of the real part of the scattering amplitude obtained in the model corresponds to the real physical situation. In the HEGS model, the real part of $F_h(s,t)$ is determined only by the complex form of energy $\hat{s} = s\ exp[-i\pi/2]$ which guarantees crossing symmetry. No other artificial function or some parameters changes the form or the s and t dependences of the real part.

Now let us include the hard pomeron in our HEGS model. In this case, the first part of the scattering amplitude, proportional to the electromagnetic form factor, gets the additional term of eq.(5) with $\epsilon_{hp} = 0.4$ and $\alpha'_{hp} = 0.1$
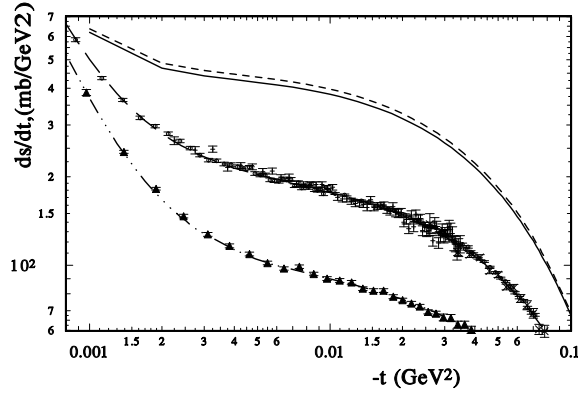
9

Figure 6: $d\sigma/dt$ in $p\bar{p}$ elastic scattering in the Coulomb-hadron interference region at $\sqrt{s} = $ 52.6 and 541 ,GeV (dash-dotted and long-dashed lines: fit of the model) and experimental data [34, 35, 36, 37]; predictions of the model for pp elastic scattering at 7 TeV (solid line) and 8 TeV (dashed line).

GeV^{-2}. First, let us examine the impact of the hard-pomeron contribution in the Coulomb-hadron interference region. In Fig. 7, the solid line represents the prediction of the model at 8 TeV. If we add the hard pomeron to the part of the Born amplitude proportional to the electromagnetic form factor and take the constants $h_{hpom.} = h_{spom.}/250$, as in [14], we obtain a large $d\sigma/dt$ (short dashed line in Fig. 7). Now let us multiply the Born amplitude by some correction factor to obtain the same differential cross sections as in the model without the hard pomeron contribution at the point $-t = 0.1$. $d\sigma/dt$ will than be smaller than the standard prediction of the model. Hence, the form of the differential cross sections in the Coulomb-hadron interference region is sensitive to the contribution of the hard pomeron. Furthermore, a measurement of $d\sigma/dt$ in this region will probe a possible contribution of the hard pomeron.

Now let us make the new fit in the whole examined region $52.8 \le \sqrt{s} \le$ 1960 GeV, including the Coulomb-hadron interference region and the large-momentum-transfer region $0.0008 \le |t| \le 9.75$ GeV^2 with the additional contribution of the hard pomeron. If we take the fixed values $\epsilon_{hp} = 0.4$ and $\alpha'_{hp} = 0.1$ GeV^{-2} and force h_{hp} to be positive, the fitting procedure gives
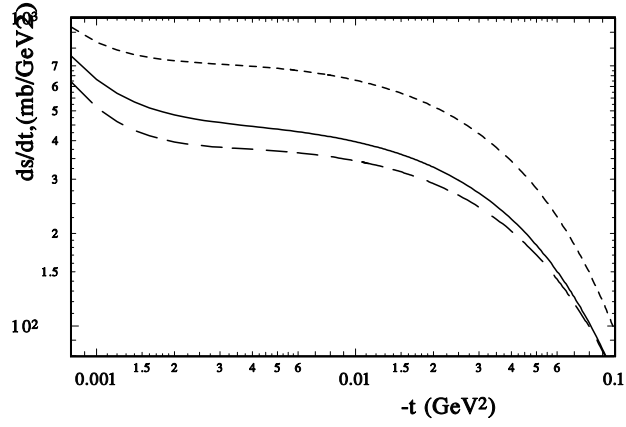
Figure 7: $d\sigma/dt$ at $\sqrt{s} = 8$ TeV: solid line - (a) the predictions of the model; short-dashed line - (b) with an additional contribution from the hard pomeron; long-dashed line - the same as the case (b) but with a normalization of $d\sigma/dt$ as in case (a) at $-t = 0.1$ GeV^2 -).

11

h_{hp}, GeV^{-2}	ϵ_{hp}	α'_{hp}, GeV^{-2}	$\sum_{i=1}^{N} \chi_i^2$
$0. \pm 0.01$	$0.4 - fixed$	$0.1 - fixed$	1783
-0.008 ± 0.001	$0.4 - fixed$	$< 0.$	1713
-0.02 ± 0.01	0.33 ± 0.04	$< 0.$	1698
-0.012 ± 0.01	$0.4 - fixed$	0.08 ± 0.01	1731

Table 1: Basic parameters of the model determined by fitting experimental data.

zero for the value of h_{hp} (see the first row in Table 1). In all other cases presented in Table 1 the fitting procedure gives a negative size for the hard pomeron constant h_{hp} and its slope tends to zero. Hence such an additional contribution plays the role of some artificial correction function and is not related with the hard pomeron contribution.

4. Conclusion

As a result, we can conclude that the unitarization procedure (example-eikonal representation) drastically changes the sum of the soft and hard pomeron contributions with momentum transfer (Fig. 7). The impact of the contribution of the hard pomeron has to be felt in most part in the Coulomb-hadron interference region and in the region of the diffraction dip.

In the framework of the HEGS model, we analyzed the possible contribution of the hard pomeron to elastic hadron scattering at LHC energies. As the amplitude of the hard pomeron has a large real part, it will have an important impact on the form of the differential cross sections in the Coulomb-hadron interference region and in the region of the diffraction minimum. The model is very simple from the viewpoint of the number of parameters and functions. There are no artificial functions or some cuts which limit the separate parts of the amplitude to some region of momentum transfer. In the framework of this model the quantitative description of all existing experimental data at $52.8 \leq \sqrt{s} \leq 1960$ GeV, including the CNI region and the large-momentum-transfer region ($0.0008 \leq |t| \leq 9.75$ GeV^2), is obtained with only 3 parameters at high energy. Hence, the model is very sensitive to any additional contribution.

The analysis of the hard pomeron contribution in the framework of this model shows that such a contribution is not felt. In most part, the fitting

procedure requires a negative additional hard pomeron contribution. Of course, the inclusion in the model of some other correction terms such as the odderon and the spin-flip amplitude can change this result. However, in that case it will be difficult to separate the hard pomeron contribution from the additional correction terms with the true energy and momentum transfer dependence. This will depend on the accuracy of the experimental data at LHC energies, especially in the CNI region where, as we have shown, the contribution of the hard pomeron is important. Of course, the final answer to the hard pomeron contribution to the elastic proton-proton scattering can be given by the LHC experiment at 14 TeV only. But up to now we can conclude that there is little space for the hard pomeron contribution in the existing experimental data on the elastic proton-proton and proton-antiproton scattering.

References

[1] A.Martin, F. Cheung, Analytic properties and bounds of the scattering amplitude (Cordon and Breach, New York, 1970).

[2] S.M.Roy, Phys.Rep. **C 5** (1972) 125 .

[3] G. Latino et all. (TOTEM Coll.), arXiv: 1110.1008.

[4] The TOTEM Collaboration (G. Antchev et al.) EPL, **95** (2011)41001.

[5] C. Bourrely, J. Soffer, T.T. Wu, Eur.Phys.J. **C28** (2003) 97.

[6] R. Fiore, L. Jenkovszky, R. Orava, E. Predazzi, A. Prokudin, O. Selyugin, Int. J. Mod.Phys., A24: 2551-2559 (2009).

[7] J. R. Cudell and O. V. Selyugin, Czech. J. Phys. **54** (2004) A441 [arXiv:hep-ph/0309194].

[8] O. V. Selyugin, J. R. Cudell and E. Predazzi, Eur. Phys. J. (ST) **162** (2008) 37 [arXiv:0712.0621 [hep-ph]].

[9] V. Uzhinsky, arXiv: 1203.3949.

[10] C. Merino and Yu.M. Shabelski, arXiv:1204.0769.

[11] I.M. Dremin and V.A. Nechitailo, arXiv:1202.2016.

[12] J. R. Cudell, E. Martynov, O. V. Selyugin and A. Lengyel, Phys. Lett. B **587** (2004) 78 [arXiv:hep-ph/0310198].

[13] A. Donnachi, P.V. Landshoff, arXiv:1112.2485

[14] A. Donnachi, P.V. Landshoff, Phys.Lett. **B387** (1996) 637.

[15] O.V. Selyugin and J.-R. Cudell, Czech. J. Phys. **54** (2004) B161.

[16] J. R. Cudell and O. V. Selyugin, Phys. Lett. B **662** (2008) 417.

[17] J. R. Cudell and O. V. Selyugin, Phys. Rev. Lett. **102** (2009) 032003 [arXiv:0812.1892 [hep-ph]].

[18] O.V. Selyugin, Eur. Phys. J. C (2012) 72:2073.

[19] O. Selyugin, O. Teryaev, Phys. Rev. D **79** (2009) 033003.

[20] O.V. Selyugin, Mod. Phys. Lett. A**9** (1994) 1207.

[21] O.V. Selyugin, Mod. Phys. Lett. A**14**, 223 (1999).

[22] O. V. Selyugin, Phys. Rev. D **60** (1999) 074028

[23] I.V. Andreev, Zh.Eksp.Theor.Fiz., **58** (1970) 253.

[24] S. Wallecc, Ann. of Phys.., **78** (1973) 190.

[25] H.M. Freid, functional Methods and Models in Quantum Field Theory (The MIT Press, Cambridge, MA 1972).

[26] R.C. Brower, M.J. Strassler and C.I. Tan, JHEP **0806** (2008).

[27] E. Levin and I. Potashnikova, arHiv:1202.1922.

[28] E. Gotsman, E. Levin and U. Maor, arXiv:1203.2419.

[29] X.D. Ji, Phys. Rev. Lett. **78** , (1997) 610; Phys. Rev D **55** (1997) 7114.

[30] Radyushkin, A.V., Phys. Rev. D **56**, 5524 (1997).

[31] H. Pagels, Phys.Rev. **144** (1966) 144.

[32] M.V. Polyakov, Phys.Lett. **B555** (2003) 57.

[33] V.M. Abazov et al. (D0 Collaboration), Phys.Rev. **D86** (2012) 012009.

[34] N.A. Amos et al. , Nucl.Phys., **B262** (1985) 689.

[35] C. Augier et al. (UA4/2 Collaboration), Phys.Lett. **B316** (1993) 448.

[36] D. Bernard et al. (UA4/1 Collaboration), Phys.Lett., **B198** (1987) 583.

[37] M. Bozzo et al., Phys.Lett., **B147** (1984) 385.